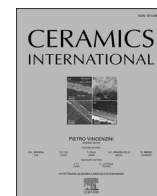




Contents lists available at ScienceDirect

Ceramics International

journal homepage: www.elsevier.com/locate/ceramint

Dielectric, electrochemical and magnetic properties of the hydrothermally synthesized double perovskite $\text{La}_2\text{NiMnO}_6$ for energy storage applications

T. Sharmili^a, A. Joana Preethi^a, J. Vigneshwaran^b, Kalaiselvan Ganesan^c, M. Ragam^{a,*}

^a Research Centre of Physics, Fatima College (Autonomous), Madurai-18, Affiliated to Madurai Kamaraj University, Madurai-21, Tamilnadu, India

^b Advanced Materials Laboratory, School of Physics, Madurai Kamaraj University, Madurai, 625021, Tamilnadu, India

^c Cavendish Laboratory, University of Cambridge, JJ Thomson Avenue, Cambridge, CB3 0HE, UK

ARTICLE INFO

Keywords:

Calcination
Dielectric properties
Electrical conductivity
Magnetic properties
Electrodes

ABSTRACT

Double perovskite materials are greatly appealing because of their multiferroic properties. Among such materials, double perovskite with rare earth metals are widely studied by researchers. Presently, the double perovskite $\text{La}_2\text{NiMnO}_6$ (LNMO) samples are synthesized using the hydrothermal method by varying the concentration of the solvent (NaOH). The Powder X-ray diffraction analysis confirmed the formation of monoclinic structure with the $\text{P2}_1/\text{n}$ space group for prepared LNMO samples. The SEM image of the prepared samples revealed a cube-like structure. The impedance, dielectric, AC conductivity and modulus are studied in a wide frequency range from 100 Hz to 5 MHz to analyse the electrical and microstructure properties of the synthesized LNMO samples. The presence of a non-Debye type of relaxation peak is confirmed by impedance, dielectric and modulus studies. The effect of grains and grain boundaries are analysed by the Nyquist plot and the polarization of the materials are explained by the Maxwell-Wagner interfacial polarization model and Koop's theory. Using a three electrode system, the electrochemical behaviour of prepared LNMO samples are studied in various concentration of electrolyte (KOH) at different scan rates and found to have a pseudocapacitive nature. The highest specific capacitance value for LNMO10 is 44.60 F/g, LNMO20 is 50.14 F/g and LNMO30 is 25.81 F/g at a scan rate of 10 mV/s for 3 M KOH. The room temperature magnetic behaviour of synthesized LNMO samples analysed by Vibrating Sample Magnetometer paves way for magnetic storage applications.

1. Introduction

The drastic development of industries and technologies in recent decades led to a serious need of energy. Most technologies, including renewable energy devices, vehicles, cell phones etc., require safe energy storage devices. For the use of clean energy sources such as solar energy, wind energy and geothermal energy, electrochemical devices like batteries, supercapacitors and fuel cells play significant roles in modern society by their revolutionary breakthroughs in science and technology [1].

Despite higher specific energy of batteries, higher cost and limited charge/discharge cycles remain challenging. As an alternative, supercapacitors are emerging as cost effective with long charge/discharge cycles. Their higher power density at extreme high temperatures turns them a promising candidate for electrochemical energy storage devices. The performance of a supercapacitor depends on the electrode and electrolyte interface, based on which it can be classified into three types:

Electric Double Layer Capacitor (EDLC), pseudocapacitor and hybrid type (combination of EDLC and pseudocapacitor). The capacitance in an EDLC is originated by the charge separation and accumulation at the electrode/electrolyte interface, whereas the pseudocapacitor stores energy by reversible redox reactions at or near the electrode/electrolyte interface [2,3]. The electrode is the main component that determines the properties of a supercapacitor, and the stability of the electrolyte determines the operating voltage window [4] that improves storage capacity [5].

In recent years, double perovskite materials are widely studied by the researchers because of their tailoring properties such as ferroelectric, dielectric, magnetic and optical. Double perovskite materials have the general formula $\text{AA}'\text{B}_2\text{O}_6/\text{A}_2\text{BB}'\text{O}_6$ (Where A is an alkaline earth metal and B is the transition metal). Liu et al. reported that $\text{PrBaMn}_2\text{O}_{6-\delta}$ (r-PBM) has a layered double perovskite structure that exhibits ultrahigh capacitance with a high gravimetric capacitance of 1034.8 F/g and a volumetric capacitance of 2535.3 F cm^{-3} at a current density of 1 A g^{-1}

* Corresponding author.

E-mail address: mraagam.physics@gmail.com (M. Ragam).

<https://doi.org/10.1016/j.ceramint.2023.11.047>

Received 6 April 2023; Received in revised form 10 October 2023; Accepted 2 November 2023

Available online 7 November 2023

0272-8842/© 2023 Elsevier Ltd and Techna Group S.r.l. All rights reserved.

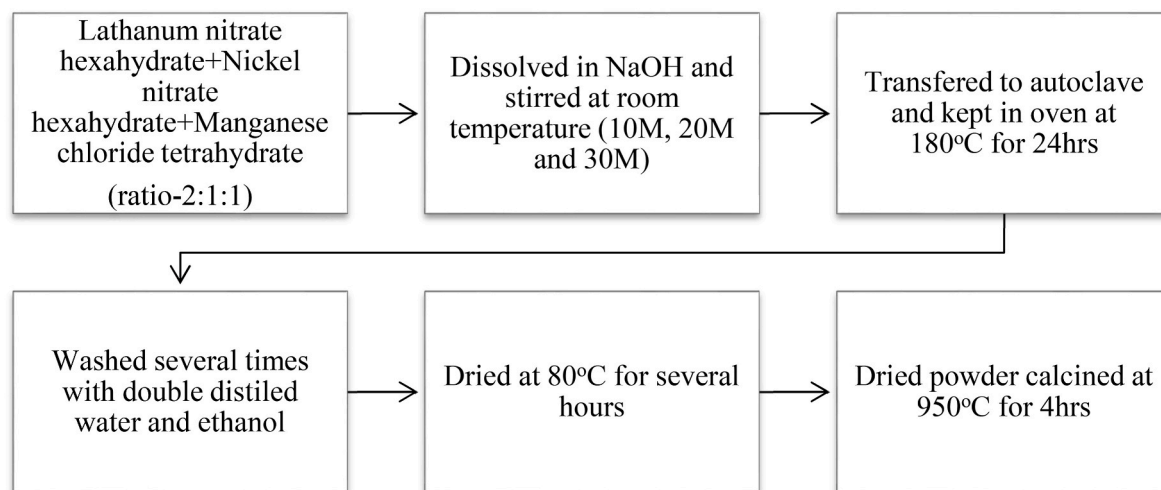


Figure-1. Preparation method for LNMO samples.

and functions as an excellent oxygen anion-intercalation-type electrode material for supercapacitors [3]. A photoelectrochemical cell for solar energy storage using halide double perovskite $\text{Cs}_2\text{AgBiBr}_2$ with a potential gain of 500 mV is achieved by Prabhu et al. [6]. Ritter et al. explored the structural and magnetic properties of $\text{AA}'\text{FeMoO}_6$ ($\text{AA}' = \text{Ba}_2, \text{BaSr}, \text{Sr}_2$ and Ca_2) and found a remarkable correlation between the Curie temperature and the electronic bandwidth [7]. Among all the double perovskite materials, R_2NiMnO_6 is unique and rarely reported. Mohd et al. investigated the R_2NiMnO_6 double perovskite by changing the A-site rare earth metal from lanthanum to yttrium and established a correlation among lattice parameters, structural distortion, octahedral tilting, superexchange angle, electronic band gap, Curie temperature, and the rare-earth ionic radius [8]. Lan et al. synthesized $\text{La}_2\text{NiMnO}_6$ and reported a bandgap value of about 1.4 eV [9]. The occurrence of a spin-lattice coupling in the $\text{RE}_2\text{NiMnO}_6$ ($\text{RE} = \text{La}, \text{Pr}, \text{Sm}$ and Tb) is reported by Lekshmi et al. [10]. Great attention is developed among researchers on R_2NiMnO_6 double perovskite materials due to its multi-ferroic behaviour. Li et al. synthesized $\text{La}_2\text{NiMnO}_6$ using sol-gel method and established the dependence of electric field on the dielectric constant [11]. The solid state reaction method for the synthesis of $\text{La}_2\text{NiMnO}_6$ is carried out by Yuan et al. [12]. Recent studies by Gaikwad et al. [13] and Kang et al. [14], reported single phase $\text{La}_2\text{NiMnO}_6$ nanorods synthesized using hydrothermal method, with higher band gap exhibiting ferromagnetic transition at 178 K and 5 K respectively with higher saturation magnetization values and magnetic moment. Presently, $\text{La}_2\text{NiMnO}_6$ is synthesized using hydrothermal method and their properties are analysed for energy storage applications.

Earlier, double perovskite Y_2NiMnO_6 (YNMO), is synthesized by hydrothermal route and its properties pertaining to energy storage was investigated and reported [15]. YNMO system is improved further by incorporating lanthanum in A-site, which has a higher ionic radius than yttrium. During the synthesis, the concentration of NaOH is varied to control the morphologies of the prepared samples to improve its electrochemical properties. Impedance, dielectric, AC conductivity, modulus and magnetic properties of the synthesized materials are investigated.

2. Experimental procedure

2.1. Synthesis procedure

In this work, $\text{La}_2\text{NiMnO}_6$ (LNMO) double perovskites are prepared using the hydrothermal method (Fig-1). For the synthesis of LNMO10, $\text{La}(\text{NO}_3)_3 \cdot 6\text{H}_2\text{O}$, $\text{Ni}(\text{NO}_3)_2 \cdot 6\text{H}_2\text{O}$ and $\text{MnCl}_2 \cdot 4\text{H}_2\text{O}$ are taken as starting materials in the ratio of 2:1:1, which is dissolved in a 10 M NaOH

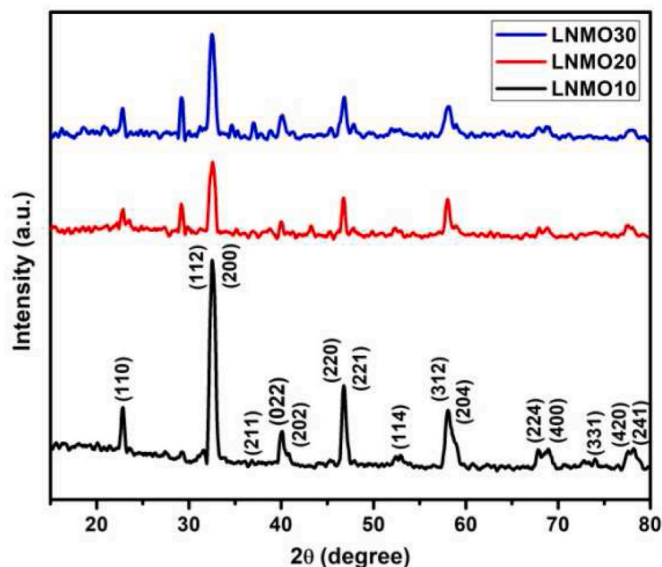


Figure-2. X-Ray Diffraction pattern of LNMO samples.

solution and stirred continuously at room temperature. The former solution is transferred to a 50 ml Teflon lined autoclave and heated at 180 °C for 24 h. Then, it is allowed to cool down naturally for some time and washed several times with deionised water and ethanol. Further it is dried at 80 °C for several hours in a hot air oven and calcined at 950 °C for 4 h. To remove the impurities, the calcined powder is washed with dilute nitric acid and dried to get the final sample. Depending on the stoichiometric ratio of La, Ni and Mn various samples (LNMO10, LNMO20 and LNMO30) are prepared.

2.2. Electrode fabrication

The synthesized double perovskite LNMO10 powder is fabricated as an electrode by mixing the electrochemically active material (LNMO10) with carbon black (a conductive material) and polyvinylidene fluoride (a binder) in a weight ratio of 80:10:10. Few drops of N-methyl-2-pyrrolidone (an organic solvent) are added to the mixture to make slurry. The final product is cast uniformly on the commercially available nickel foam (area-1cm²×1cm²) and it is dried in an oven at 80 °C for 2 h [16]. Same procedure is followed to prepare LNMO20 and LNMO30 electrodes. The fabricated electrodes are used to study its electrochemical

Table-1

Crystallite size (D), Dislocation density (δ) and Lattice strain (ϵ) of LNMO samples calculated using Scherrer equation.

LNMO-NaOH	Crystallite size, D (nm)	Dislocation density, $\delta \times 10^{-3} \text{ (nm}^{-2}\text{)}$	Lattice strain, $\epsilon \text{ (lines/m}^2\text{)}$
LNMO10	34.78	2.8	4.74
LNMO20	33.49	2.9	3.97
LNMO30	26.39	3.7	5.14

studies.

3. Structural characterization

3.1. X-ray diffraction spectroscopy

The prepared samples X-ray diffraction are recorded at room temperature using an X-Ray powder Diffractometer (PANalytical, $\lambda = 1.5418 \text{ \AA}$) with $\text{CuK}\alpha$ radiation in Bragg's angle (2θ), with a wide range of $20\text{--}80^\circ$ (fig-2). For all the three prepared samples, some of the diffraction peaks observed at 2θ values are 22.8° , 32.7° , 39.9° , 46.7° , 58° , 68.5° and 77.6° that correspond to the diffraction planes of (110), (112), (220), (312), (224) and (116). The obtained peaks are consistence with the reported results, and they belong to the monoclinic structure with a space group $\text{P2}_1/\text{n}$ [17]. The structure of the perovskite material is identified by the Goldschmidt factor or tolerance factor (t) given by,

$$t = \frac{r_{\text{La}} + r_{\text{O}}}{\sqrt{2} \left(\frac{r_{\text{Ni}} + r_{\text{Mn}}}{2} + r_{\text{O}} \right)} \quad (1)$$

Here, r_{La} , r_{Ni} , r_{Mn} and r_{O} denote the ionic radii of lanthanum, nickel, manganese and oxide, respectively. According to the tolerance factor (t), if the value of 't' is equal to or close to 1 then it undergoes cubic structure. If the value is less than 0.97, the structure is distorted and may belong to monoclinic or orthorhombic structure. Here, the ionic radii of lanthanum, nickel, manganese and oxygen are 1.36, 0.69, 0.64 and 1.4 respectively. Therefore, the calculated t value is 0.94, which is lesser than 0.97. As a result, it is confirmed that it undergoes monoclinic structure [18].

Using Scherrer equation [19], the average crystallite size (D), dislocation density (δ) and lattice strain (ϵ) for synthesized LNMO10, LNMO20 and LNMO30 are calculated and listed in the table-1. The dislocation density is the number of dislocations per unit area of the crystalline material that is inversely proportional to the crystallite size or particle size. Lattice strain is the measure of distribution of lattice constants, such as lattice dislocation and this may be due to the imperfections in the sample [20]. From Table-1 it is inferred that due to the higher supersaturation, crystallite size (D) decreases with an increase in concentration of NaOH. Supersaturation is one of the main reasons for crystal nucleation and growth. At lower supersaturation, crystal growth

Table-2

Crystallite size (D_{WH}) and Microstrain (ϵ_{WH}) of LNMO samples using W-H plot.

LNMO-NaOH	Crystallite size, D_{WH} (nm)	Microtrain, $\epsilon_{\text{WH}} \times 10^{-3}$
LNMO10	25.30	8.34
LNMO20	24.98	8.06
LNMO30	28.88	8.58

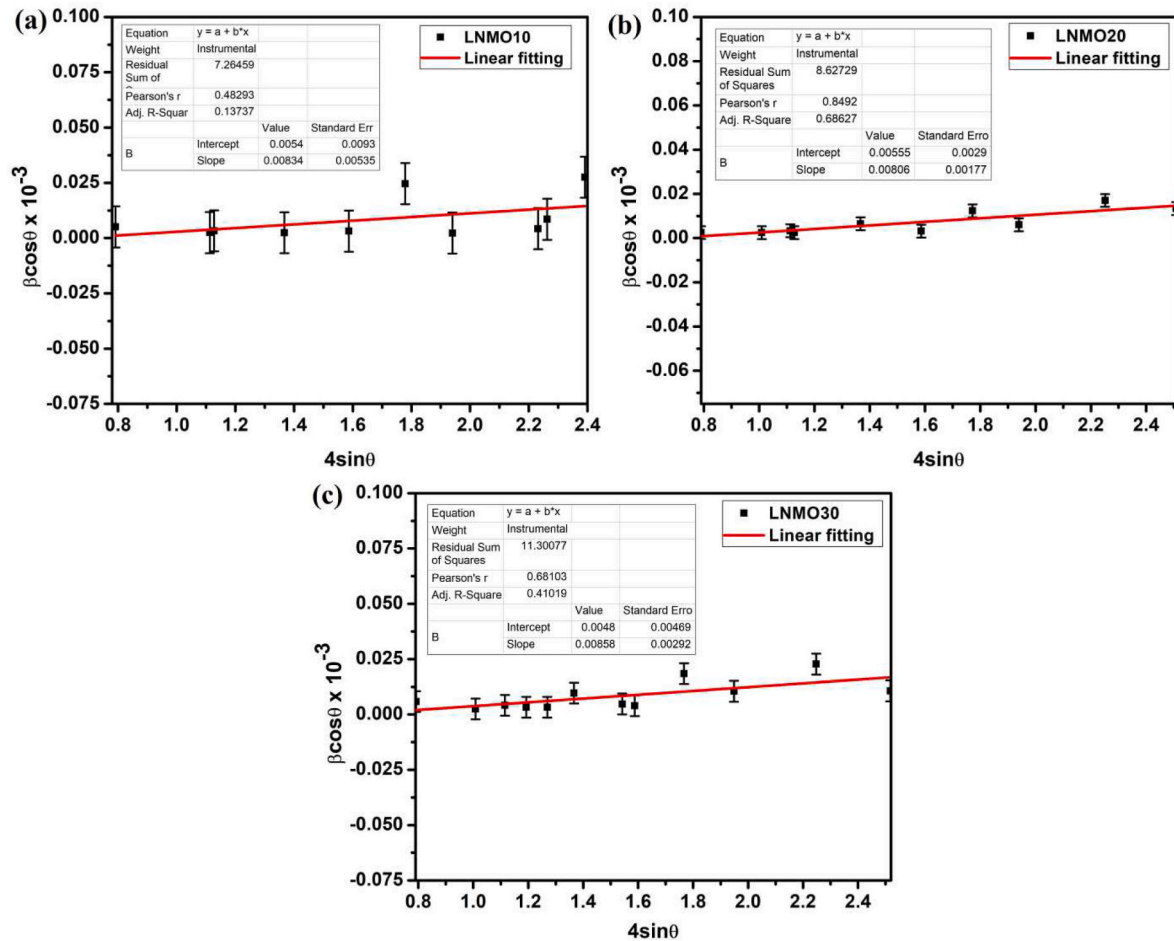


Fig-3. (a, b and c): The Williamson-Hall plot for prepared LNMO samples.

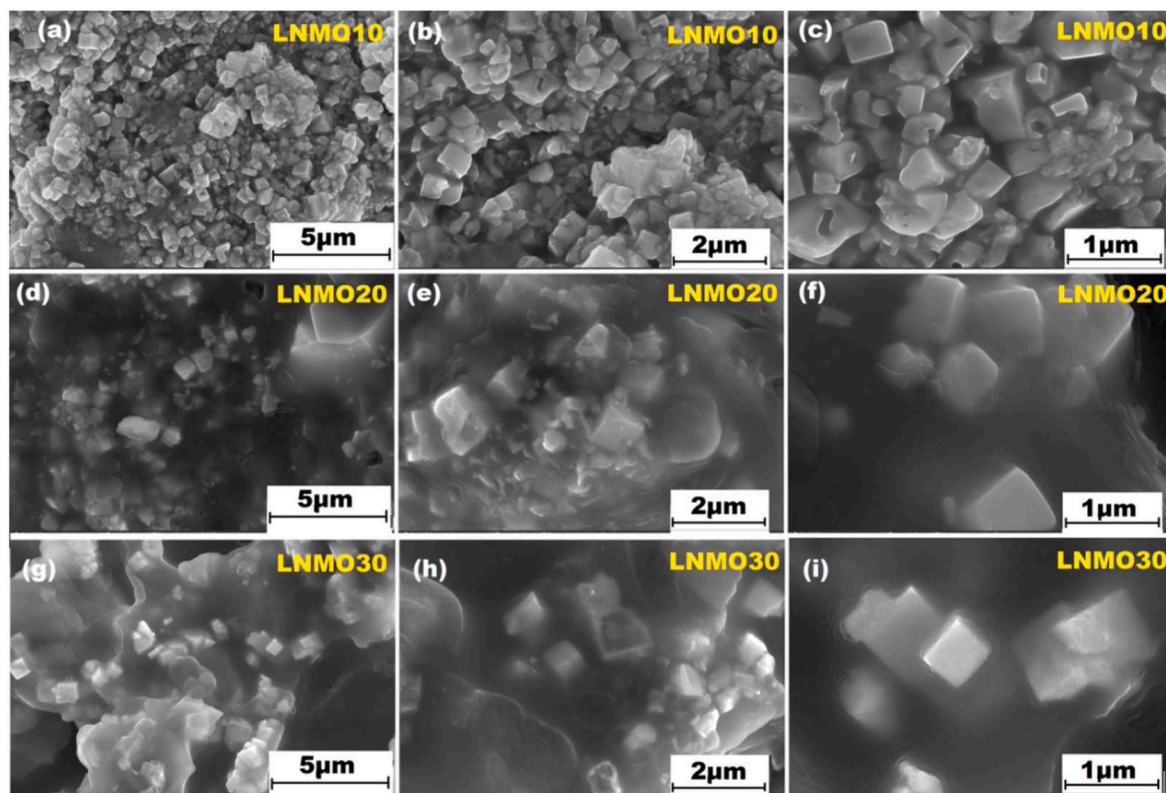


Figure-4. SEM analysis of LNMO samples at different magnifications.

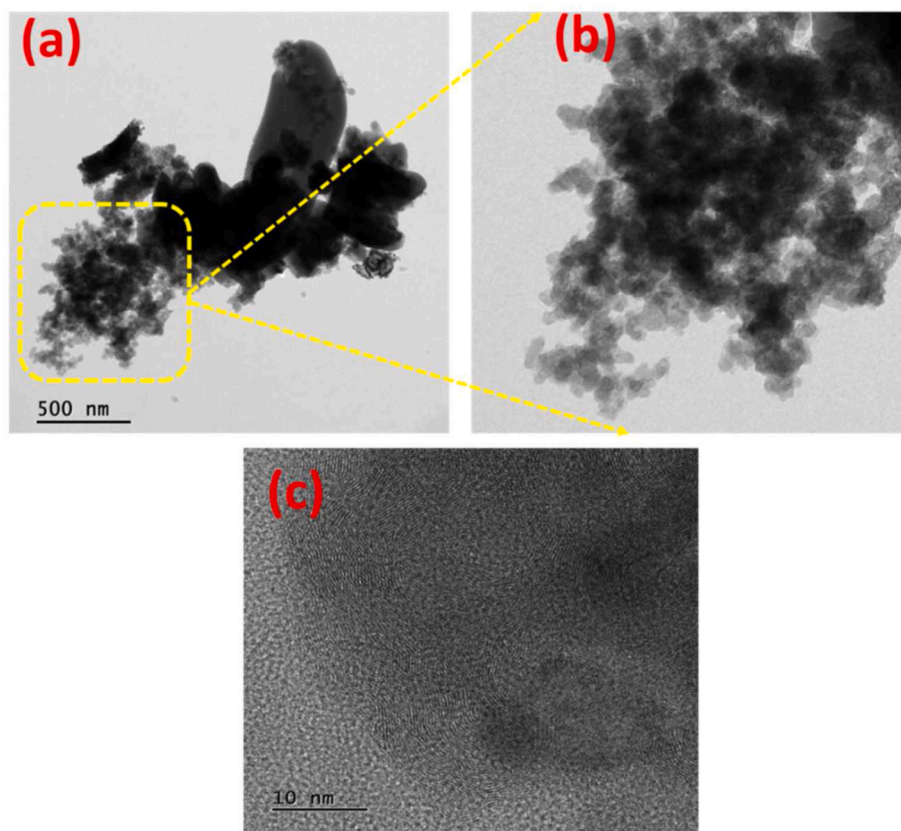


Fig. 5(a). HRTEM images of synthesized $\text{La}_2\text{NiMnO}_6$ (LNMO-20) sample, (b) Magnified images of synthesized $\text{La}_2\text{NiMnO}_6$ (LNMO-20) and (c) Highly magnified images regularly oriented $\text{La}_2\text{NiMnO}_6$ (LNMO-20) in uniaxial direction.